

## **Astrophysical Spectropolarimetry and Magnetic Field Diagnostics**

J. Trujillo Bueno

*Instituto de Astrofísica de Canarias, 38200 La Laguna, Tenerife, Spain*

### **Abstract.**

This paper highlights the increasing interest of astrophysical spectropolarimetry by showing how remote sensing techniques based on the Hanle and Zeeman effects are allowing us to investigate the magnetism of the extended solar atmosphere. Particular emphasis is given to the development of new diagnostic windows on the weakest magnetic fields of the photosphere, chromosphere and corona. Spectropolarimetry in the He I 10830 Å multiplet is allowing us to infer the three-dimensional geometry of the magnetic fields that confine the plasma of solar prominences. Multilevel modelling of the Hanle and Zeeman effects in the Ca II IR triplet and other chromospheric lines is helping us to decipher the strength and topology of chromospheric magnetic fields in regions where photospheric magnetograms show the well-known 'salt and pepper' patterns of mixed polarities. The Hanle effect in molecular lines, as well as in atomic lines of rare-earth elements like Ce II, offers a novel diagnostic tool for empirical investigations of 'turbulent' magnetic fields in relatively deep regions of the 'quiet' solar photosphere.

### **1. Introduction**

As pointed out in the preface to the book on *Astrophysical Spectropolarimetry* (Trujillo Bueno et al. 2002a), the polarization of light is the key to unlocking new discoveries and obtaining the information we need to understand the physics of many phenomena occurring in the Universe. Particularly relevant examples, besides the magnetized plasmas of the Sun and peculiar A- and B-type stars, are young stellar objects and their surrounding disks, symbiotic stars, stellar winds, active galactic nuclei, black hole jets, magnetized neutron stars, X-ray pulsars, the interstellar medium, the cosmic microwave background radiation and its cosmological implications, etc. Spectropolarimetry provides powerful diagnostics of the physical conditions in astrophysical plasmas, for instance, concerning magnetic fields, which cannot be obtained via conventional spectroscopy. Moreover, since completely unpolarized radiation can be expected only from a perfectly symmetric object, it may also help us to verify the geometry of the astrophysical system under investigation, even without being possible to resolve it spatially.

---

<sup>1</sup>Consejo Superior de Investigaciones Científicas; Spain

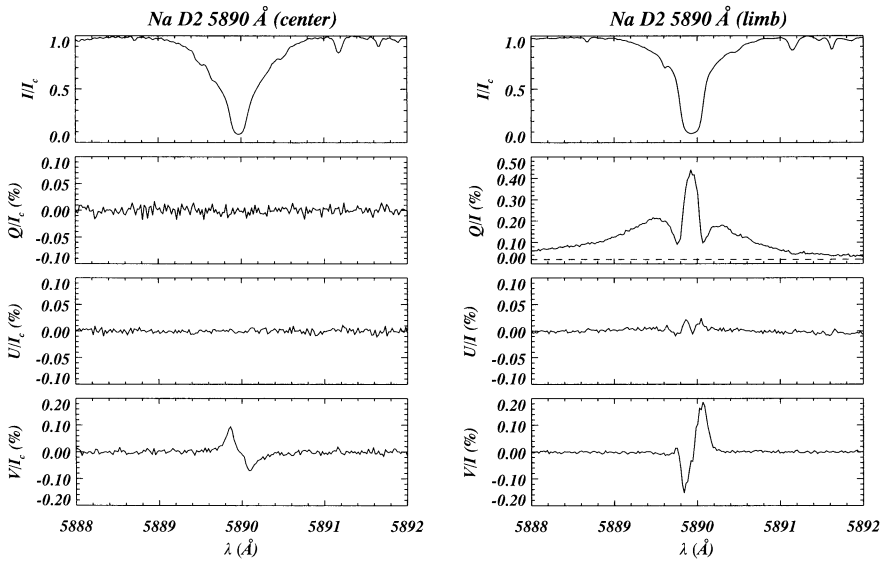


Figure 1. The full Stokes vector of the Na I D<sub>2</sub> line observed with the telescope THÉMIS in very ‘quiet’ regions of the solar atmosphere. Left panel: solar disc center. Right panel: at about 5” from the solar north limb and with the spectrograph’s slit parallel to it. The disk-center figure shows the Stokes profiles normalized to the local continuum intensity, while the solar limb figure shows the fractional polarization (i.e.,  $X(\lambda)/I(\lambda)$ ; with  $X = Q, U, V$ ). The reference direction for  $Q > 0$  is as indicated in Figure 2. From Trujillo Bueno *et al.* (2001).

Spectropolarimetry is being used with great success in solar physics. Although its application to other fields of astrophysics is still at an early stage of development, it is actually becoming increasingly attractive. This is mainly due to the observational opportunities opened up by the new generation of ground-based and space-borne telescopes as well as to recent advances in the theory and numerical modelling of the generation and transfer of polarized radiation in magnetized plasmas. This paper highlights the increasing interest of astrophysical spectropolarimetry by illustrating how remote sensing techniques based on the Hanle and Zeeman effects are allowing us to investigate the weak magnetism of the solar atmosphere.

## 2. The Zeeman effect, optical pumping and the Hanle effect

In stellar atmospheres, the most important mechanisms that induce (and modify) polarization signatures in spectral lines are the Zeeman effect, anisotropic radiation pumping and the Hanle effect (e.g. Trujillo Bueno 2001). All these physical mechanisms leave their ‘fingerprints’ in the polarization of the electromagnetic radiation that we collect with our increasingly large telescopes. The interesting point is that the development of diagnostic techniques that combine

the Hanle and Zeeman effects in suitably chosen spectral lines may allow us to investigate the strength and topology of stellar magnetic fields in a parameter domain which ranges from at least milligauss to many thousands of gauss.

The Zeeman effect requires the presence of a magnetic field, which causes the atomic and molecular energy levels to split into different magnetic sublevels. This Zeeman splitting produces local *sources* and *sinks* of light polarization because of the ensuing wavelength shifts between the  $\pi$  and  $\sigma$  transitions. The Zeeman effect is most sensitive in *circular* polarization (quantified by the Stokes  $V$  parameter), with a magnitude that for not too strong fields scales with the ratio between the Zeeman splitting and the width of the spectral line (which is very much larger than the natural width of the atomic levels), and in such a way that the emergent Stokes  $V(\lambda)$  profile changes its sign for opposite orientations of the magnetic field vector. This so-called *longitudinal* Zeeman effect responds to the line-of-sight component of the magnetic field. Accordingly, if we have a perfect cancellation of mixed magnetic polarities within the spatio-temporal resolution element of the observation, the measured circular polarization would be exactly zero *if* the thermodynamic and dynamic properties of the mixed magnetic components are similar.

In contrast, the *transverse* Zeeman effect responds to the component of the magnetic field perpendicular to the line of sight, but produces *linear* polarization signals (quantified by the Stokes  $Q$  and  $U$  parameters) that are normally below the noise level of present observational possibilities for intrinsically weak fields (i.e. with  $B < 100$  gauss). Note that in spectropolarimetric observations at the very center of the solar disk vertical fields produce zero linear polarization, independently of whether or not we have mixed magnetic polarities. However, in observations at other heliocentric angles (e.g. at  $\mu = \cos\theta = 0.5$ ) vertical fields with opposite polarities could be detected via the transverse Zeeman effect, simply because the Stokes  $Q$  profile is invariant to a reversal of the transverse field direction if the magneto-optical effects are negligible (Stenflo 1994; see also Landi Degl'Innocenti & Landi Degl'Innocenti 1981). For example, with the Tenerife Infrared Polarimeter developed by the IAC such a detection should be feasible for vertical fields with sufficient filling factor and strengths  $B > 100$  gauss. Similarly, horizontal fields with random azimuth within the resolution element of the observation give zero linear polarization at the center of the solar disk, while such fields could in principle be detected via the transverse Zeeman effect in observations close to the solar limb.

The Stokes  $V(\lambda)$  profiles shown in Fig. 1 are mainly due to the longitudinal Zeeman effect. However, the physical origin of the observed *linear* polarization signals has nothing to do with the transverse Zeeman effect. They are due to *atomic polarization*, i.e. to the existence of population imbalances and quantum interferences (or coherences) among the sublevels pertaining to the upper and/or lower atomic levels involved in the line transition under consideration. This *atomic level polarization* results from radiative transitions induced by an *anisotropic radiation field*.

As illustrated in Fig. 2, the atoms and molecules in a stellar atmosphere are illuminated *anisotropically* (see also Fig. 5 in Trujillo Bueno 2001). The mere presence of population imbalances among the sublevels of degenerate levels implies local *sources* and *sinks* of linear polarization, even in the absence

**ANISOTROPIC ILLUMINATION**

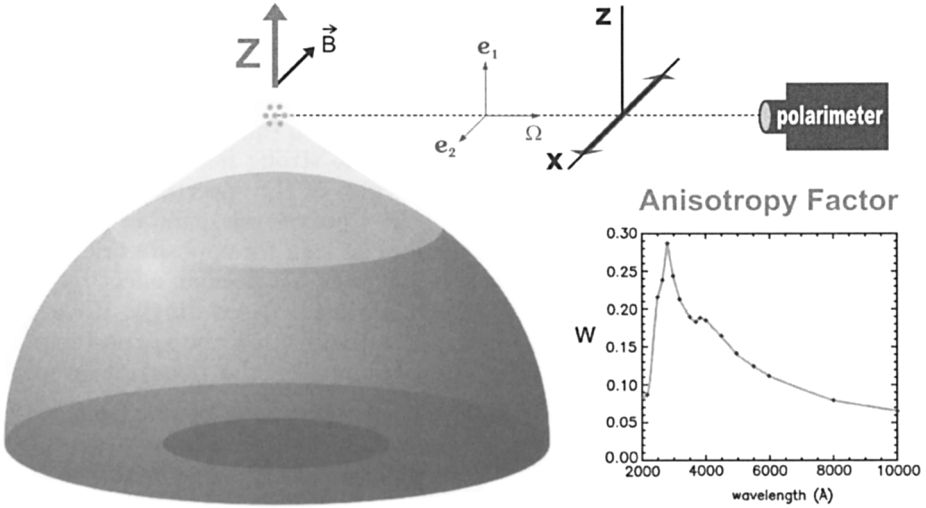


Figure 2. Anisotropic illumination of the outer atmospheric layers of a stellar atmosphere. The ‘degree of anisotropy’ of the incident radiation field is quantified by  $\mathcal{A} = J_0^2/J_0^0$ , where  $J_0^0$  is the familiar *mean intensity* and  $J_0^2 \approx \oint \frac{d\vec{\Omega}}{4\pi} \frac{1}{2\sqrt{2}} (3\mu^2 - 1) I_{\nu, \vec{\Omega}}$  (where  $I_{\nu, \vec{\Omega}}$  is the specific intensity -i.e. the Stokes-*I* parameter- as a function of frequency  $\nu$  and direction  $\vec{\Omega}$ , while  $\mu = \cos \theta$ , with  $\theta$  the polar angle with respect to the Z-axis). The possible values of the ‘anisotropy factor’  $W = \sqrt{2} \mathcal{A}$  vary between  $W = -1/2$ , for the limiting case of illumination by a purely horizontal radiation field without any azimuthal dependence, and  $W = 1$ , for purely vertical illumination. It is important to point out that the larger the ‘anisotropy factor’ the larger the fractional atomic polarization that can be induced, and the larger the amplitude of the emergent linear polarization (see the review by Trujillo Bueno 2001, and note that there is a typing error in his Eq. (11), which is correct for  $2\mathcal{A}$  and *not* for  $\mathcal{A}$ , as it was typed). We choose the positive direction for the Stokes *Q* parameter along the X-axis, i.e. along the perpendicular direction to the stellar radius vector through the observed point. The inset shows the wavelength dependence of the anisotropy factor corresponding to the center to limb variation of the observed solar continuum radiation. Note that  $W \approx 0.14$  at 5000  $\text{\AA}$ . Interestingly, the maximum anisotropy factor occurs around 2800  $\text{\AA}$ , i.e. very near the central wavelengths of the *h* and *k* lines of Mg II, whose polarization may contain valuable information on the magnetic fields and physical conditions of the solar transition region. This strongly suggests that we should urgently put a good UV polarimeter in a space telescope.

of magnetic fields. A useful formula to estimate the emergent fractional polarization at the core of a spectral line for an observation along the line of sight specified by  $\mu$  is (Trujillo Bueno 1999; 2002):

$$Q/I \approx \frac{3}{2\sqrt{2}}(1 - \mu^2)[\mathcal{W}\sigma_0^2(\text{up}) - \mathcal{Z}\sigma_0^2(\text{low})], \quad (1)$$

where  $\sigma_0^2 = \rho_0^2/\rho_0^0$  quantifies the *fractional atomic alignment* or *degree of population imbalance* of the upper or lower levels of the line transition under consideration, while  $\mathcal{W}$  and  $\mathcal{Z}$  are simply numbers which depend on the total angular momentum values of both levels (e.g.  $\mathcal{W} = \mathcal{Z} = -1/2$  for a transition with  $J_l = J_u = 1$ ). For example, a level with total angular momentum  $J = 1$  has three magnetic sublevels with individual populations denoted by  $N_i$ ; for this level  $\rho_0^2 = (N_1 - 2N_0 + N_{-1})/\sqrt{6}$  and  $\rho_0^0 = (N_1 + N_0 + N_{-1})/\sqrt{3}$ , so that  $\sigma_0^2 = 0$  if the three sublevels turn out to be equally populated. Thus, the scattering polarization  $Q/I = 0$  if  $\sigma_0^2 = 0$  in the upper and lower levels of the spectral line under consideration. In Eq. (1) the  $\sigma_0^2$  values are those corresponding to the optical depth  $\tau$  where  $\tau/\mu \approx 1$  (which means  $\tau = 0$  for a limb observation at  $\mu = 0$ ). Eq. (1) can be used for estimating the amplitude of the emergent scattering polarization in relatively strong spectral lines, either for the case of an unmagnetized stellar atmosphere or for a stellar atmospheric model with a microturbulent and isotropically distributed magnetic field. It is indeed a very useful formula because it shows clearly that the observed fractional polarization in a given spectral line has in general two contributions: one from the fractional alignment of the upper-level ( $\sigma_0^2(u)$ ) and an extra one from the fractional alignment of the lower level ( $\sigma_0^2(l)$ ). In general, the first contribution (caused exclusively by the emission events from the polarized upper level) is the only one that is normally taken into account. However, the second contribution (caused by the selective absorption resulting from the population imbalances of the lower level) plays the key role in producing the ‘enigmatic’ linear polarization signals that have been discovered recently in ‘quiet’ regions close to the solar limb, as well as in solar coronal filaments (see the reviews by Trujillo Bueno 1999, 2001; see also Trujillo Bueno & Landi Degl’Innocenti 1997; Manso Sainz & Trujillo Bueno 2001; Trujillo Bueno & Manso Sainz 2002; Trujillo Bueno et al. 2002b).

The observed polarization signals are weak because the ‘degree of anisotropy’ of the solar radiation field is weak (which leads to population imbalances and coherences that are small compared with the overall population of the atomic level under consideration), but also because we have collisions and magnetic fields which tend to modify the atomic polarization. The Hanle effect is the modification of the atomic-level polarization (and of its ensuing observable effects on the emergent linear polarization) caused by the action of a weak magnetic field (see the review by Trujillo Bueno, 2001). As the Zeeman sublevels of degenerate atomic levels are split by the magnetic field, the degeneracy is lifted and the coherences (and, in general, also the population imbalances among the sublevels) are modified. Therefore, the Hanle effect is sensitive to magnetic fields such that the corresponding Zeeman splitting is comparable to the inverse lifetime (or natural width) of the lower or the upper atomic levels of the line transition under consideration. For the Hanle effect to operate, the magnetic field vector ( $\mathbf{B}$ ) has to be significantly *inclined* with respect to the symmetry axis of the pumping

radiation field. The basic approximate formula to estimate the magnetic field intensity  $B_H$  (measured in gauss) to which the Hanle effect can (in principle) be sensitive is

$$8.79 \times 10^6 B_H g_J \approx 1/t_{\text{life}}, \quad (2)$$

where  $g_J$  and  $t_{\text{life}}$  are, respectively, the Landé factor and the lifetime (in seconds) of the atomic level under consideration (which can be either the upper or the lower level of the chosen spectral line). This formula shows that the measurement and physical interpretation of weak polarization signals in suitably chosen spectral lines may allow us to diagnose magnetic fields having intensities between  $10^{-3}$  and 100 gauss approximately, *i.e.*, in a parameter domain that is very hard to study via the Zeeman effect alone. As illustrated in Fig. 3 of Trujillo Bueno (2002), the Hanle effect in photospheric molecular lines offers a promising diagnostic window for the empirical exploration of magnetoconvection in the solar photosphere (see also Fig. 5 below).

### 3. Photospheric Magnetism: Zeeman and Hanle Diagnostics

This section considers various diagnostic windows for the empirical investigation of the distribution of magnetic fields in the ‘quiet’ solar photosphere, with particular emphasis on how to derive Probability Density Functions or PDFs (see, e.g., Emonet & Cattaneo 2001 for PDFs that result from numerical simulations of the interaction between turbulent convection and magnetic fields). The Cumulative Distribution Function (CDF), or fractional volume occupied by fields of strength smaller than  $B$  (cf. Stenflo 1999), can be suitably obtained by integrating the PDF. The PDF gives the probability of finding a magnetic intensity between  $B$  and  $B + dB$ .

#### 3.1. Zeeman diagnostics in the near IR

When one uses the Zeeman effect as diagnostic tool of the quiet Sun magnetic fields (e.g. Lin & Rimmele 1999; Sánchez Almeida & Lites 2000; Khomenko et al. 2002), one is able to obtain very useful empirical information like that given in Fig. 3. It shows histograms of the line-of-sight component of the magnetic field as obtained directly from the Zeeman splittings measured in some of the several classes of Stokes  $V$  profiles we have observed under extraordinary seeing conditions on July 29, 2000 in a disk-center inter-network region using the Tenerife Infrared Polarimeter. Only ‘normal’ Stokes  $V$  profiles with a positive and a negative lobe have been used (*i.e.* these histograms do not include the extra information provided by the ‘anomalous’ Stokes  $V$  profiles with three lobes observed in about 40% of the pixels). These histograms confirm that the photospheric plasma of the ‘quiet’ Sun has a *continuous distribution of magnetic field strengths*, from the kilogauss range to at least 300 gauss. All these ‘quiet-Sun’ magnetic fields that have been detected via the Zeeman effect seem to occupy a very small fraction of the photospheric volume (*i.e.* the inferred filling factors are of the order of a few percent, only). Note that the histogram corresponding to the granular pixels (dashed-line) has its peak at 300 G with a sudden (artificial) decrease towards smaller field strengths, while the inter-granular histogram (dotted line) peaks at about 500 G and does not show such a sudden cutoff. Clearly,

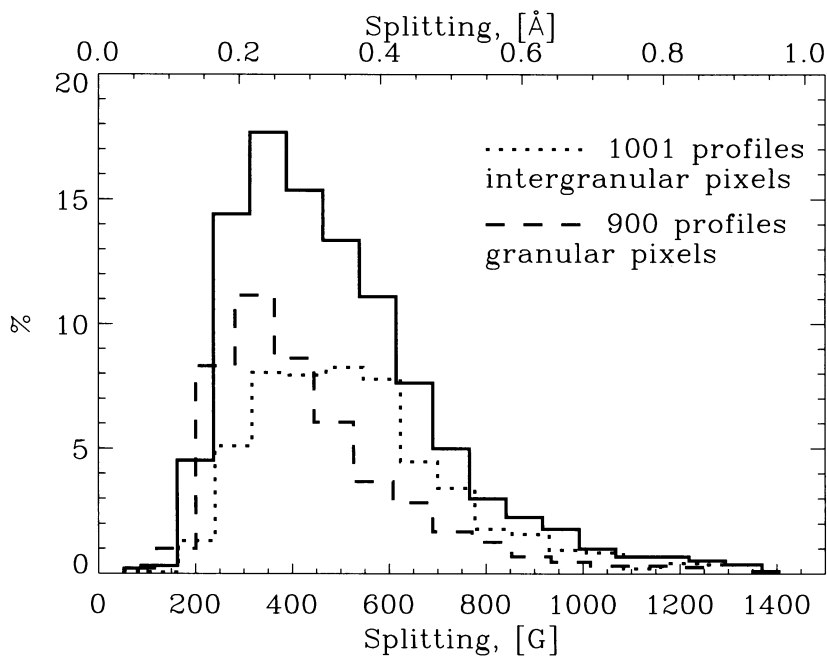


Figure 3. Histograms of the observed Zeeman splittings in some of the various classes of Stokes  $V$  profiles observed at the solar disk center in a very quiet inter-network region using the Fe I lines at  $1.56\mu\text{m}$ , and distinguishing between granular and inter-granular pixels. From Khomenko et al. (2002).

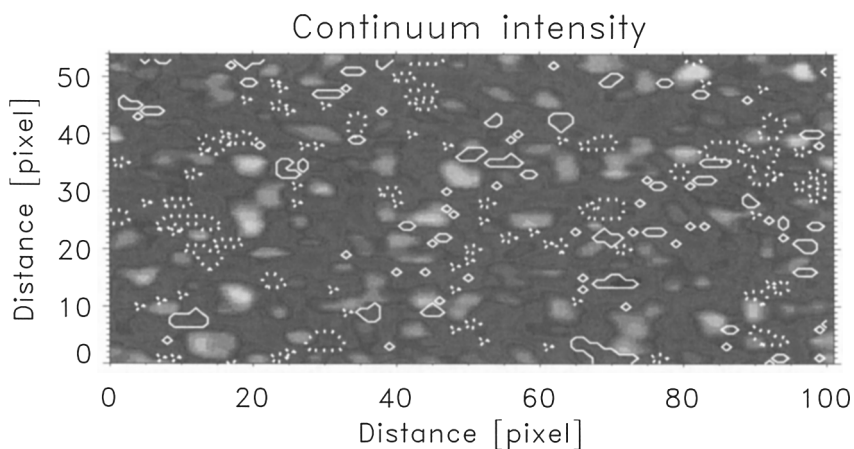


Figure 4. The shaded image represents the map of solar granulation over which are plotted contours showing the location of the class 4 Stokes  $V$  profiles discussed in the text. Solid and dotted lines indicate opposite magnetic polarities.

the magnetic field tends to be stronger in the inter-granular lanes than above the bright granular areas (as seen in continuum intensity). Interestingly, the larger the downflow velocity the stronger the field, while the weakest fields tend to be located in the upflowing regions. Finally, it is important to point out that the peak at about 350 G in the total solid-line histogram (or Probability Density Function) is artificial since it is produced by both the limited spatial and temporal resolutions of the observations (1" and 1 minute, respectively) and by the limited Zeeman sensitivity of the chosen Fe I lines at  $1.56\ \mu\text{m}$ . Actually, both general physical arguments and the magnetoconvection simulations shown at this conference by Cattaneo and by Stein & Nordlund suggest that the PDF should actually continue increasing towards very weak fields. The weaker the field the easier the possibility of having highly tangled field lines with the result of mixed polarities at small spatial scales.

The eight classes of Stokes  $V$  profiles found by Khomenko et al. (2002) for the  $1.56\ \mu\text{m}$  Fe I lines can be used for new investigations on some interesting points. Fig. 4 shows a very recent result obtained in collaboration with Elena Khomenko (Main Astronomical Observatory; Kiev). The contours show the inter-granular locations where happen to be situated just one of the eight discovered Stokes- $V$  classes for the IR lines. The selected class corresponds to Stokes  $V$  profiles with two lobes showing the largest observed splittings and a red-shift in their zero-crossing. This class of Stokes  $V$  profiles is seen in only 15% of the total number of pixels that show circular polarization above the noise level. Moreover, note that they are situated in some (but not all) of the inter-granular lanes. It will be interesting to investigate whether or not the observed locations of the magnetic fields which lead to this and other classes of Stokes  $V$  profiles correspond mainly to the boundaries of the meso-granular scale cells, as it happens to occur for the relatively few kilogauss fields that arise in the magnetoconvection simulations for weak seed-field values shown at this conference by Stein & Nordlund.

### 3.2. The Hanle effect in the Sr I 4607 Å line.

How could we investigate empirically the weak-field part of the PDF (e.g. for  $B < 100$  gauss)? The Hanle effect may well have the required diagnostic potential (e.g. Stenflo 1994), but the problem is how to apply it to obtain reliable information given that a Hanle-effect diagnostics relies on a comparison between the observed linear polarization and that calculated for the zero-field reference case. Fig. 4 in Trujillo Bueno (2001) demonstrates that the 'degree of anisotropy' of the radiation field sensitively depends on the source function gradient of the spectral line under consideration: the larger the gradient the larger the anisotropy. In a forthcoming paper, Shchukina & Trujillo Bueno will show how 'dangerous' can be a Hanle-effect diagnostics of a mixed-polarity weak field, when this diagnostics is based on scattering polarization calculations of the Sr I 4607 Å line in *one-dimensional* semi-empirical models of the solar atmosphere. However, these authors conclude that a reliable diagnostics can indeed be achieved by means of *three-dimensional* (3D) scattering polarization calculations in snapshots taken from the time-dependent hydrodynamical simulations of solar surface convection described by Asplund et al. (2000). The computed 'degree of anisotropy' of the strontium line radiation shows a considerable horizontal fluctuation at

all heights in the 3D model. The fluctuation in the emergent fractional linear polarization ( $Q/I$ ) is also very significant. We find that both, upflowing and downflowing regions contribute to the emergent fractional polarization for the  $B = 0$  G reference case. The spatially and temporally averaged Stokes profiles give a  $Q/I$  that is *lower* than that calculated in one-dimensional semi-empirical atmospheric models, but it is still a bit larger than the observed  $Q/I$ , thus indicating the need of invoking a depolarizing mechanism.

Multilevel Hanle-effect calculations in snapshots taken from ‘realistic’ simulations of magnetoconvection for different values of the assumed seed field will be helpful to end up with a more accurate knowledge of the distribution of magnetic fields in weakly magnetized regions of the solar photosphere. Note that the Hanle field for the Sr I line at  $\lambda 4607 \text{ \AA}$  is  $B_H \approx 23 \text{ G}$  (see Eq. 2). Because of the high intermittency of the photospheric magnetic field, we expect that the largest Hanle depolarization will take place in the downflowing regions at the boundaries of the meso-granular and granular scales. Therefore, a Hanle effect diagnostics assuming a microturbulent field with strength independent of the horizontal position *will be biased towards magnetic strengths smaller than those which are actually producing the observed Hanle depolarization*. Finally, it is important to emphasize that one should ideally use several spectral lines simultaneously. A good choice is the linearly polarized spectrum of Ti I, which has been studied recently by Manso Sainz & Landi Degl’Innocenti (2002).

### 3.3. The Hanle effect in molecular lines

The empirical PDF that we are obtaining via 3D scattering polarization simulations of the observed polarization in the Sr I 4607  $\text{\AA}$  line corresponds to relatively high regions of the quiet solar photosphere (i.e. around 400 km for observations at  $\mu = 0.1$ ). Is there any possibility of a reliable empirical investigation of the weak field part of the PDF, but at considerably deeper photospheric regions ?

Figure 5 shows a practical estimation of the ‘upper-level Hanle fields’ calculated with Eq. (2) for the lines of the P and R branches of  $C_2$  molecules, which show beautiful scattering polarization signatures on the Sun (see the atlas of Gandorfer 2000). Because the Landé factors of the upper-levels of the  $R_2$  ( $P_2$ ) lines are much smaller than those of the  $R_1$  ( $P_1$ ) and  $R_3$  ( $P_3$ ) lines, the magnetic field strength needed for a significant Hanle-effect suppression of the scattering polarization signal is considerably smaller for the  $R_1$  ( $P_1$ ) and  $R_3$  ( $P_3$ ) lines than for the  $R_2$  ( $P_2$ ) lines. For example, for  $C_2$  lines of the R branch with total angular momentum  $30 < J < 40$  our estimation of the Hanle field lies between only 4 and 8 gauss for the  $R_1$  and  $R_3$  lines, but between 100 and 200 gauss for the  $R_2$  lines. This very sizable difference in the sensitivity to the Hanle effect between the  $R_2$  lines (which are blended with the  $R_1$  lines) and the  $R_3$  lines is being used by us for constraining the weak-field part of the solar ‘magnetoturbulent spectrum’ in relatively deep regions of the solar photosphere. As it can be seen in Gandorfer’s (2000) atlas, the ratio ( $\mathcal{R}$ ) of the observed fractional polarizations between  $R_2$  lines and  $R_3$  lines is  $\mathcal{R} \approx 2$ , concerning those  $R_2$  lines which are perfectly blended with  $R_1$  lines. However, a detailed investigation of the scattering polarization in such molecular lines taking into account the overlapping effect between the  $R_1$  and  $R_2$  lines shows that there is no significant magnetic depolarization of the  $R_3$  lines with respect to the  $R_2$  lines. Actually, if there

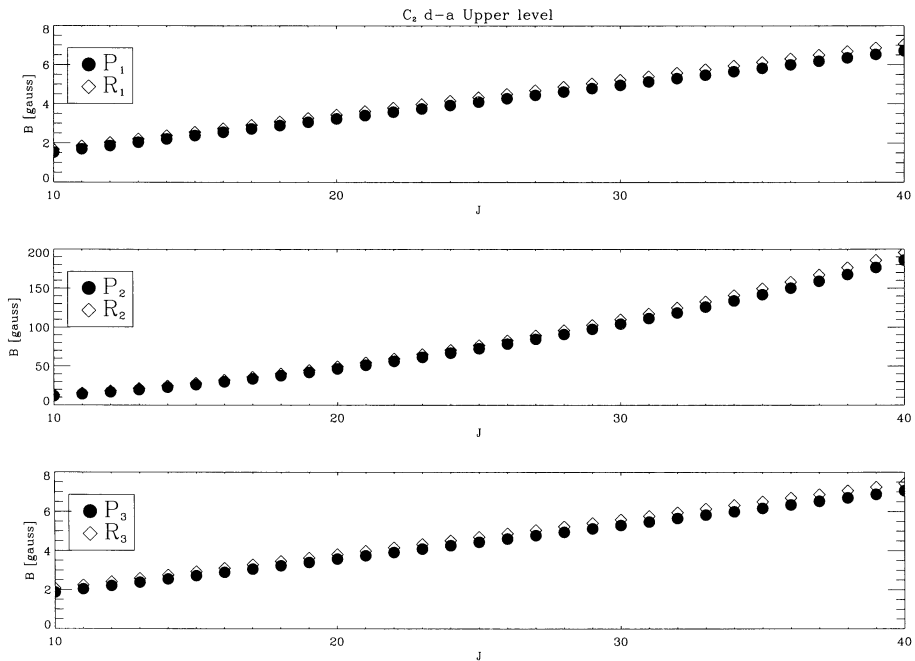


Figure 5. Application of the basic formula of the Hanle effect (see Eq. 2) to the upper levels of C<sub>2</sub> lines taking  $t_{\text{life}} \approx 1/A_{J_u J_l}$ , with  $A_{J_u J_l}$  the Einstein coefficient of the P or R line under consideration. Although this approximation leads to a subestimation of the upper-level Hanle fields by about a factor of 2, the magnetic strengths given here are actually indicating the intensity of a ‘turbulent’ field that would be sufficient to produce a significant modification of the scattering polarization amplitudes. Each point refers to a spectral line of the P or R branches, whose lines with lower-level angular momentum  $J_l = J$  have  $J_u = J - 1$  and  $J_u = J + 1$ , respectively. Note that the Hanle field is much larger for P<sub>2</sub> (R<sub>2</sub>) lines than for P<sub>1</sub> (R<sub>1</sub>) and P<sub>3</sub> (R<sub>3</sub>) lines.

were a significant magnetic depolarization the above-mentioned ratio  $\mathcal{R}$  would then be larger than 2, which is not observed. Therefore, only a relatively small fraction of the volume occupied by the photospheric regions that are effective in producing the observed molecular polarization can be filled with magnetic fields of strength similar or larger than the above-mentioned ‘Hanle fields’ of the R<sub>1</sub> and R<sub>3</sub> lines. But, which photospheric regions contribute to the observed linear polarization in molecular lines?

It is very important to realize that molecular lines are indeed sensitive to the Hanle effect, because the Landé factor of their lower and upper levels, although small, is non-zero. The fact that the ‘Hanle field’ in Fig. 5 increases with  $J$  is simply the result of the corresponding decrease of the Landé factor, as it can be deduced directly from the ensuing formula for Hund’s case (b) given by Landau & Lifshitz (1982), which offers a good approximation for  $J > 10$ . Therefore, the

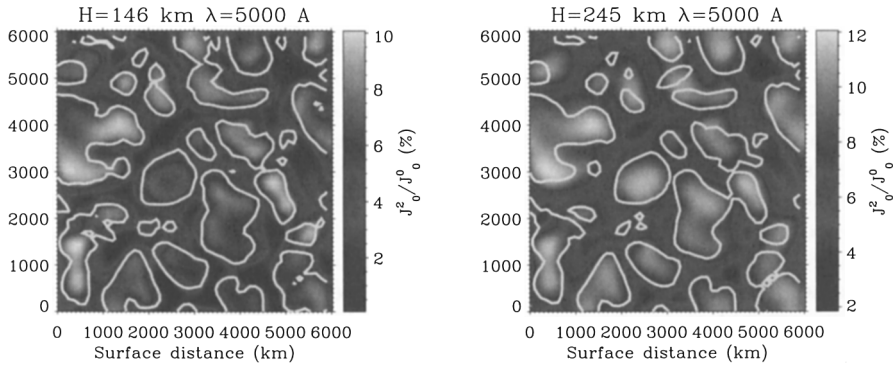


Figure 6. The horizontal variation of the degree of anisotropy of the solar continuum radiation at  $5000 \text{ \AA}$  calculated at two heights in a snapshot taken from a realistic hydrodynamical simulation of solar surface convection. The solid lines delineate upflowing regions. Note that in this range of heights where the  $C_2$  lines are ‘formed’ (concerning simulated observations at  $\mu = 0.1$ ), there is a clear correlation between the upflowing regions and the degree of anisotropy of the continuum radiation. Moreover, there is also a significant correlation with the horizontal fluctuation of the molecular number density.

explanation of the interesting observational fact reported by Gandorfer (2001) and by Berdyugina, Stenflo & Gandorfer (2002) that in quiet-Sun regions close to the solar limb the scattering polarization amplitudes of molecular lines remain practically invariant over the years is *not* because molecular lines are ‘magnetically insensitive’ or ‘immune to the Hanle effect’, as claimed by those authors, but because the observed scattering polarization in molecular lines is coming *mainly from the upflowing regions of the solar photosphere where the weakest magnetic fields tend to be located*. In fact, as we shall show in a forthcoming publication, the central part of our empirically-determined PDF turns out to be very narrow, implying that *most of the upflowing photospheric volume can only be occupied by very weak fields*. This important conclusion is supported by Fig. 6, which shows that the weakly magnetized upflowing regions are precisely the locations where the anisotropy factor of the solar continuum radiation is the largest.

### 3.4. The Hanle effect in atomic lines of rare earth elements

The very same fact illustrated in Fig. 6 helps to explain why the scattering polarization observations reported by Stenflo & Keller (1997) and by Gandorfer (2000; 2002) show significant polarization peaks in spectral lines of the rare earth elements (e.g. Nd II at  $\lambda 5249.57$ , Yb I at  $\lambda 3987.96$ , Eu II at  $\lambda 4129.72$ , Ce II at  $\lambda 4062.23$ , Ce II at  $\lambda 4083.22$ , etc.). The solar abundance of these chemical elements is extremely low (e.g.  $N_{\text{Ce}}/N_{\text{H}} \sim 10^{-11}$ ). However, their transitions have sizable Einstein coefficients for the spontaneous emission process (e.g.  $A_{ul} \approx 10^8 \text{ s}^{-1}$  and  $A_{ul} \approx 6 \times 10^7 \text{ s}^{-1}$  for the above-mentioned Ce II lines, re-

spectively) and they show interesting scattering polarization signals of great diagnostic potential (e.g. the upper-level Hanle fields for those Ce II lines are  $B_H \approx 14$  G and  $B_H \approx 6$  G, respectively). Rare earth ions like Ce II have a very high density of levels whose populations seem to be determined by interlockings through radiative excitations and de-excitations (Canfield 1971). It is of great scientific interest to model the scattering polarization in the spectral lines of rare earth elements. At present, the first choice for us is Ce II, because it produces clean polarization peaks above and below the level of continuum polarization in several transitions and because it has no hyperfine structure splitting, which facilitates the ensuing modelling problem. Interestingly, the Ce II lines which show linear polarization peaks *above* the level of continuum polarization have  $J_l = J_u$ . There is a beautiful physical explanation for this observational fact.

#### 4. Chromospheric Magnetism: Hanle and Zeeman Diagnostics

As we have seen, most of the photospheric surface is occupied by the 'quiet' inter-network regions of mixed polarity fields and we have lots of good reasons to wish to know how important is the degree of intermittency of the chromospheric field (see, e.g., Title's keynote paper in this volume; see also Trujillo Bueno & Manso Sainz 2002). Do chromospheric field lines result mainly from the extension of the underlying mixed polarity field of the 'quiet' solar photosphere? Or is the chromospheric field dominated by the field lines from the boundaries of the supergranulation network? The true empirical answer to this type of questions is encoded in the polarization of chromospheric spectral lines.

A serious problem is that chromospheric lines like the Ca II IR triplet are relatively broad, which implies that the weak magnetic fields of the 'quiet' chromospheric regions are very difficult to diagnose via the only consideration of the longitudinal Zeeman effect on which magnetograms are based on. Fortunately, in recent years, observational investigations of scattering polarization on the Sun have pointed out the existence of 'enigmatic' linear polarization signals in several spectral lines observed in the 'quiet' solar chromosphere close to the solar north pole, which cannot be understood in terms of the classical theory of scattering polarization (Stenflo and Keller, 1997; Stenflo, Keller & Gandorfer, 2000). These 'enigmatic' features of the linearly-polarized solar-limb spectrum have motivated novel theoretical investigations of scattering polarization, which are now making feasible reliable confrontations between spectropolarimetric observations and multilevel radiative transfer simulations of the Hanle and Zeeman effects (see the reviews by Trujillo Bueno 1999, 2001, 2002; see also Trujillo Bueno & Manso Sainz 2002). Such investigations have been carried out within the framework of the quantum theory of line formation (Landi Degl'Innocenti 1983), which allows us to formulate scattering polarization problems taking into account a key physical ingredient that had been previously neglected: ground-level atomic polarization (i.e. the existence of population imbalances and/or coherences among the Zeeman sublevels of the lower-level of the spectral line under consideration).

Let us consider the modelling issue of the 'enigmatic' linear polarization signatures of the Ca II IR triplet observed by Stenflo et al. (2000) in 'quiet' regions close to the solar limb. This topic has been investigated in detail by Manso Sainz & Trujillo Bueno (2001) and by Trujillo Bueno & Manso Sainz (2002), who have

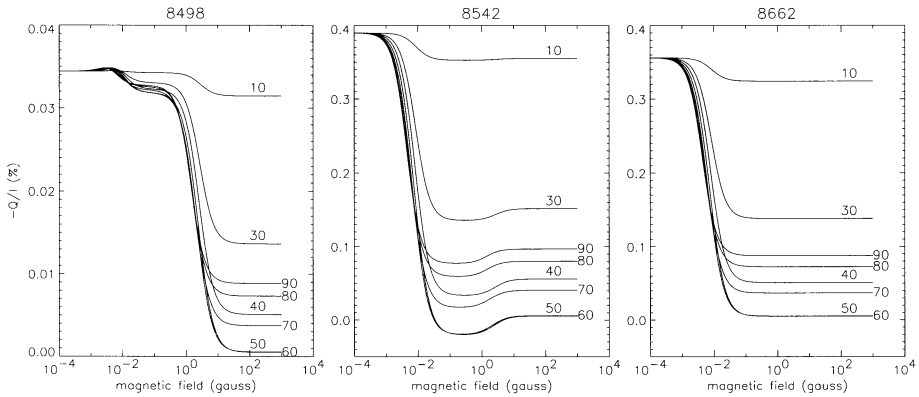


Figure 7. The fractional linear polarization of the Ca II IR triplet calculated at  $\mu = 0.1$  (about  $5''$  from the limb) in an isothermal model of the solar chromosphere. Each curve corresponds to the indicated inclination ( $\theta_B$ ) of the assumed random-azimuth magnetic field. From Trujillo Bueno & Manso Sainz (2002).

developed a general multilevel scattering polarization computer program for the numerical simulation of the Hanle and Zeeman effects in weakly magnetized stellar atmospheres. Firstly, we considered the zero magnetic field reference case and demonstrated that the ‘enigmatic’  $Q/I$  amplitudes observed by Stenflo et al. (2000) are the natural consequence of the existence of sizeable amounts of population imbalances in the metastable levels  $^2D_{3/2}$  and  $^2D_{5/2}$  (which are the *lower-levels* of the Ca II IR triplet). Secondly, we have investigated the Hanle effect in the IR triplet at 8498, 8542 and 8662 Å considering a realistic multilevel atomic model. Fig. 7 shows the fractional linear polarization calculated at  $\mu = 0.1$  (about  $5''$  from the limb) assuming magnetic fields of given inclination, but with a random azimuthal component within the spatio-temporal resolution element of the observation.

The results of Fig. 7 are very interesting. They indicate that by comparing the observed fractional polarization amplitudes in the three IR lines, we may hope to investigate empirically whether or not milligauss fields in the ‘quiet’ solar chromosphere can have a sizable filling factor. Thus, if the  $Q/I$  line-core amplitudes of 0.035%, 0.13% and 0.12% reported by Stenflo et al. (2000) are really accurate, then we could explain them via a distribution of sub-gauss fields with pretty chaotic field lines. On the other hand, if one opts for chromospheric fields with strengths in the gauss range, then we see in Fig. 7 that there are two possible magnetic-field topologies for which the limb polarization signals of the 8542 and 8662 Å lines can have amplitudes with  $Q/I \geq 0.1\%$  (i.e. of the order of the observed ones). As one could have expected, the first topology corresponds to magnetic fields with inclinations  $\theta_B \leq 30^\circ$  (because the Hanle effect is not efficient for vertical fields). The second corresponds to magnetic fields which are practically parallel to the solar surface, i.e. ‘horizontal’ fields with  $80^\circ \leq \theta_B \leq 100^\circ$ .



with plasma in subtle ways, where dense plasma is being supported against gravity and where thermal instability is producing a cool condensation, and so by studying these fascinating objects in detail we can learn how these fundamental processes are likely to operate elsewhere in the Universe. On the other hand, the eruption of a prominence often produces a coronal mass ejection which may have a dramatic influence on near-Earth space weather.

The Tenerife Infrared Polarimeter allows us to measure the four Stokes parameters with an unprecedented degree of sensitivity in the near IR. Using this instrument attached to the German Vacuum Tower Telescope and modelling the observed spectral line polarization within the framework of the quantum theory of line formation, we are investigating the three-dimensional structure of the magnetic fields that confine the plasma of solar prominences (see our first results in Trujillo Bueno et al. 2002*b*). To this end, we have developed suitable inversion algorithms for deriving the magnetic field vector from the observed polarization in the He I 10830 multiplet. Figure 3 in the letter by Trujillo Bueno et al. (2002*b*) contrasts our theoretical modelling versus the observed Stokes profiles in one of the many prominences we have observed. Figure 8 below shows that the magnetic field vector in a prominence that was located at the solar south pole is *rotating* around a fixed direction in space (given by  $\theta_B \approx 25^\circ$  and  $\chi_B \approx 168^\circ$ ) as we move along consecutive spatial points (Merenda, Trujillo Bueno, Landi Degl'Innocenti & Collados 2002; in preparation). This is very interesting because the slit-jaw image of the observed polar prominence was actually formed by several nearly vertical threads of plasma and the spectrograph slit was crossing them at a given height above the solar limb.

## 6. Concluding remarks

Polarized light provides the most reliable source of information at our disposal for the remote sensing of astrophysical magnetic fields, including those on the Sun. Although substantial progress has been made in recent years concerning the theory and numerical modelling of the generation and transfer of polarized radiation in stellar atmospheres, we are still crying for suitable polarimeters for the present generation of 10-m class telescopes. In solar physics we have witnessed interesting observational discoveries thanks to the development of novel polarimeters like the ASP, ZIMPOL or TIP. However, in order to open a true empirical window on the magnetism of the extended solar atmosphere, we need urgently an UV polarimeter in a space telescope and a cleverly-designed large ground-based solar telescope optimized for spectropolarimetric observations, and installed on an excellent site like that chosen by Scharmer et al. (2002) for the Swedish 1-m Solar Telescope.

**Acknowledgments.** The results described here owe much to ongoing collaborations with Andrés Asensio Ramos, Manolo Collados, Elena Khomenko, Egidio Landi Degl'Innocenti, Rafael Manso Sainz, Laura Merenda and Nataliya Shchukina. Partial support by the Spanish Ministerio de Ciencia y Tecnología and by FEDER through project AYA2001-1649 is gratefully acknowledged.

## References

- Asplund, M., Ludwig, H.G., Nordlund, Å & Stein, R.F. 2000, *A&A*, 359, 669
- Berdyugina, S.V., Stenflo, J.O. & Gandorfer, A. 2002, *A&A*, 388, 1062
- Canfield, R.C. 1971, *A&A*, 10, 64
- Emonet, T. & Cattaneo, F. 2001, *ApJ*, 560, L197
- Gandorfer A. 2000, *The Second Solar Spectrum*, Vol. 1, ETH, Zürich.
- Gandorfer A. 2001, in *Advanced Solar Polarimetry*, M. Sigwarth (ed.), ASP Conf. Series, Vol. 236, 109
- Gandorfer A. 2002, *The Second Solar Spectrum*, Vol. 2, ETH, Zürich.
- Khomenko, E.V. et al. 2002, *A&A*, submitted
- Landi Degl'Innocenti, E. 1983, *Sol. Phys.*, 85, 3
- Landi Degl'Innocenti, E. & Landi Degl'Innocenti, M. 1981, *Il Nuovo Cimento*, 62, 1
- Landau, L.D. & Lifshitz, E.M. 1982, *Quantum Mechanics*, Pergamon, Oxford
- Lin, H., & Rimmele, T. 1999, *ApJ*, 514, 448
- Manso Sainz, R., & Trujillo Bueno, J. 2001, in *Advanced Solar Polarimetry*, M. Sigwarth (ed.), ASP Conf. Series, Vol. 236, 213-220.
- Manso Sainz, R., & Landi Degl'Innocenti, E. 2002, *A&A*, 394, 1093
- Priest, E.R. 1989, in 'Dynamics and Structure of Quiescent Solar Prominences', E.R. Priest (ed.), Kluwer, 1
- Sánchez Almeida & Lites, B. 2000, *ApJ*, 532, 1215
- Scharmer, G.B. et al. 2002, *Nature*, 420, 151
- Stenflo, J.O. 1994, *Solar Magnetic Fields: Polarized Radiation Diagnostics*, Kluwer Academic Publishers
- Stenflo, J.O. 1999, in *Solar Polarization*, K. N. Nagendra & J. O. Stenflo (eds.), Kluwer Academic Publishers, 1
- Stenflo, J.O., & Keller, C. 1997, *A&A*, 321, 927
- Stenflo, J.O., Keller, C., & Gandorfer, A. 2000, *A&A*, 355, 789
- Trujillo Bueno, J. 1999, in *Solar Polarization*, K. N. Nagendra & J. O. Stenflo (eds.), Kluwer Academic Publishers, 73-96
- Trujillo Bueno, J. 2001, in *Advanced Solar Polarimetry*, M. Sigwarth (ed.), ASP Conf. Series, Vol. 236, 161-195
- Trujillo Bueno, J. 2002, in *Stellar Atmosphere Modeling*, I. Hubeny, D. Mihalas & K. Werner (eds.), ASP Conf. Series, in press
- Trujillo Bueno, J. & Landi Degl'Innocenti, E. 1997, *ApJ Letters*, 482, L183
- Trujillo Bueno, J., Collados, M., Paletou, F., & Molodij, G. 2001, in *Advanced Solar Polarimetry*, M. Sigwarth (ed.), ASP Conf. Series, Vol. 236, 141
- Trujillo Bueno, J. & Manso Sainz, R. 2002, *Il Nuovo Cimento C*, Vol. 25
- Trujillo Bueno, J., Moreno Inertis, F., & Sánchez, F. (eds.) 2002a, *Astrophysical Spectropolarimetry*, Cambridge University Press
- Trujillo Bueno, J. et al. 2002b, *Nature*, 415, 403